



Dielectric relaxation behaviors of pure and Pr₆O₁₁-doped CaCu₃Ti₄O₁₂ ceramics in high temperature range

L.F. Xu, P.B. Qi, X.P. Song, X.J. Luo, C.P. Yang*

Faculty of Physics and Electronic Technology, Hubei University, Wuhan 430062, People's Republic of China

ARTICLE INFO

Article history:

Received 15 November 2010
Received in revised form 16 February 2011
Accepted 19 February 2011
Available online 5 March 2011

Keywords:

CaCu₃Ti₄O₁₂
Dielectric spectrum
Complex impedance spectrum

ABSTRACT

Pure and Pr₆O₁₁-doped CaCu₃Ti₄O₁₂ (CCTO) ceramics were prepared by conventional solid-state reaction method. The compositions and structures were characterized by X-ray diffraction (XRD) and scanning electron microscopy (SEM). The influences of Pr-ion concentration on dielectric properties of CCTO were measured in the ranges of 60 Hz–3 MHz and 290–490 K. The third phase of Ca₂CuO₃ was observed from the XRD of CCTO ceramics. From SEM, the grain size was decreased obviously with high valence Pr-ion (mixing valence of Pr³⁺ and Pr⁴⁺) substituting Ca²⁺. The room temperature dielectric constant of Pr-doped CCTO ceramics, sintered at 1323 K, was an order of magnitude lower than the pure CCTO ceramics due to the grain size decreasing and Schottky potential increasing. The dielectric spectra of Pr-doped CCTO were flatter than that of pure CCTO. The loss tangent of Pr-doped CCTO ceramics was less than 0.20 in 2 × 10²–10⁵ Hz region below 440 K. The complex impedance spectra of pure and Pr-doped CCTOs were fitted by ZView. From low to high frequency, three semicircles were observed corresponding to three different conducting regions: electrode interface, grain boundary and grain. By fitting the resistors *R* and capacitors *C*, the activation energies of grain boundary and electrode contact were calculated. All doped CCTOs showed higher activation energies of grain boundary and electrode than those of pure CCTO ceramics, which were concordant with the decreasing of dielectric constant after Pr₆O₁₁ doping.

© 2011 Elsevier B.V. All rights reserved.

1. Introduction

The giant dielectric constant material CaCu₃Ti₄O₁₂ (CCTO) has been attracting many attentions because of its intriguing mechanism and potential technical applications in microelectronic devices. CCTO shows an extremely huge dielectric constant up to 10⁵ in the ranges of dc – 10⁶ Hz and 100 – 600 K [1,2]. Some researchers suggested that this dielectric behaviour is intrinsic [2–4], while others prefer to attribute it to some extrinsic factors, such as the barrier layer capacitance effect between twin crystals [1], internal barrier layer capacitor (IBLC) mechanism between semi-conducting grains and insulating grain boundaries [5–7], internal domains inside CCTO grains [8,9], electrode polarization effects [10] and so on. It is believed that the insulating interfaces would form on semi-conducting grains during sintering process. Thus, among those factors, the IBLC and electrode polarization effects termed Maxwell–Wagner are commonly accepted. However, there is no enough evidence for their origin. Recently a multipole trap charge repositioning model [11,12] was presented, which in principle can yield a large permittivity. The analysis suggests that the

charged trap state relaxation defined by an electric monopole is the key point to understand the electrical behavior of CCTO. In addition, the orientation of dipoles developed by the trap sites, which yield a large polarization, is the second key element contributing to the giant dielectric constant of CCTO. Moreover, some people have reported first principles computations on native point defects in CCTO and elaborated on the possibility of multipole defects in CCTO [13].

In this work, we mainly focus on the variations of the permittivity spectra to explore the influences of praseodymium (Pr) doping on the properties of CCTO. It is known that the radius of the substituting element determines the incorporation site [14]. Thus Pr-ion is preferred to other ions since the radius of Pr³⁺ (1.013 Å) and Pr⁴⁺ (0.90 Å) are so close to Ca²⁺ (0.99 Å). By a traditional solid-state reaction method, various Pr-ion proportions, from Pr₆O₁₁, were doped into CCTO to synthesize Ca_{1–11x/6}Pr_xCu₃Ti₄O₁₂ (*x* = 0.00, 0.05, 0.10, 0.15 and 0.20). Thereafter, the influences of Pr-ion doping on dielectric properties and microstructures of CCTO were investigated.

2. Experimental procedure

The Ca_{1–11x/6}Pr_xCu₃Ti₄O₁₂ (*x* = 0.00, 0.05, 0.10, 0.15 and 0.20, abbreviated as CCTO, PCCTO-1, PCCTO-2, PCCTO-3 and PCCTO-4, respectively) pellets were prepared using a solid-state reaction and sintering process. The raw materials: CaCO₃ (99%), TiO₂ (99.0%), CuO (99.0%) and Pr₆O₁₁ (99.99%) were directly combined in the

* Corresponding author. Tel.: +86 027 88665447; fax: +86 027 88663390.
E-mail address: cpyang@hubu.edu.cn (C.P. Yang).

necessary stoichiometric ratio. Thorough mixing was achieved by milling the powders in ethanol for no less than 4 h. The dried mixtures were calcined at 1223 K (950 °C) for 10 h before being milled a second time. Then, the dried powders were ground for 4 h in ethanol and then uniaxially cold pressed into pellets with 12 mm diameter and thickness about 1 mm under 14 MPa. The brown pellets were then sintered in air using the schedule 10 K/min to 1323 K (1050 °C), 12 h hold, and then furnace cooled to room temperature.

The X-ray diffraction (XRD) patterns of sintered samples were obtained in a range of 10–80° at room temperature, in a Japan D/Max-3C system, with Cu K α radiation ($\lambda = 0.1506$ nm) at 35 kV and 25 mA, with a step of 10°/min. Microstructures of the fractured surfaces were examined using a scanning electron microscope (SEM, s-4800, Japan). The dielectric properties and impedance spectra were determined on samples with opposite sides painted with silver paste, using a WK6420 impedance analyzer with a Janis closed-cycle-refrigerator from 60 Hz to 3 MHz under 290–490 K.

3. Results and discussion

Fig. 1 illustrates XRD patterns of the sintered $\text{Ca}_{1-11x/6}\text{Pr}_x\text{Cu}_3\text{Ti}_4\text{O}_{12}$ ($x = 0.00, 0.05, 0.10, 0.15$ and 0.20) ceramics. Except for the main phase CCTO, peaks of CuO could also be observed from Pr-ion concentration 0.00 to 0.15. This kind of segregation was also observed by Prakash and Varma [15]. For higher concentrations as $x = 0.20$, XRD patterns show the presence of the third phase identified as Ca_2CuO_3 , which could be caused by the reaction of excess Ca^{2+} and Cu-ion on grain boundaries.

Fig. 2 illustrates SEM images of the samples. The morphology of undoped CCTO sample consists of some huge grains

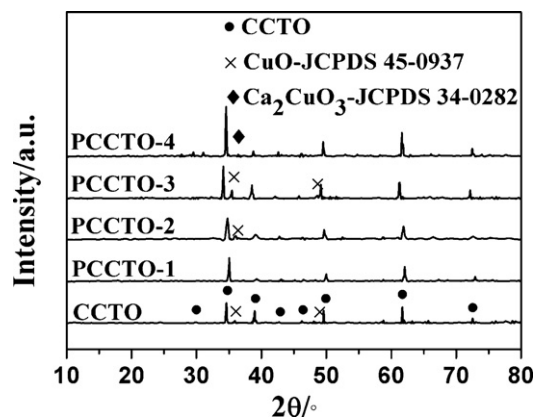


Fig. 1. X-ray diffraction patterns for CCTO and PCCTO ceramics.

(50–100 μm), surrounded by small ones (~ 2 μm). PCCTO ceramics have more uniform little grains of 1–5 μm . All doped samples show an extremely grain size decreasing. When the content of praseodymium increases, both the number and size of large grains would decrease.

Fig. 3 illustrates variations of dielectric constant ϵ' with frequency at a few selected temperatures for undoped CCTO and PCCTOs ($x = 0.05, 0.10, 0.15$ and 0.20). At room temperature

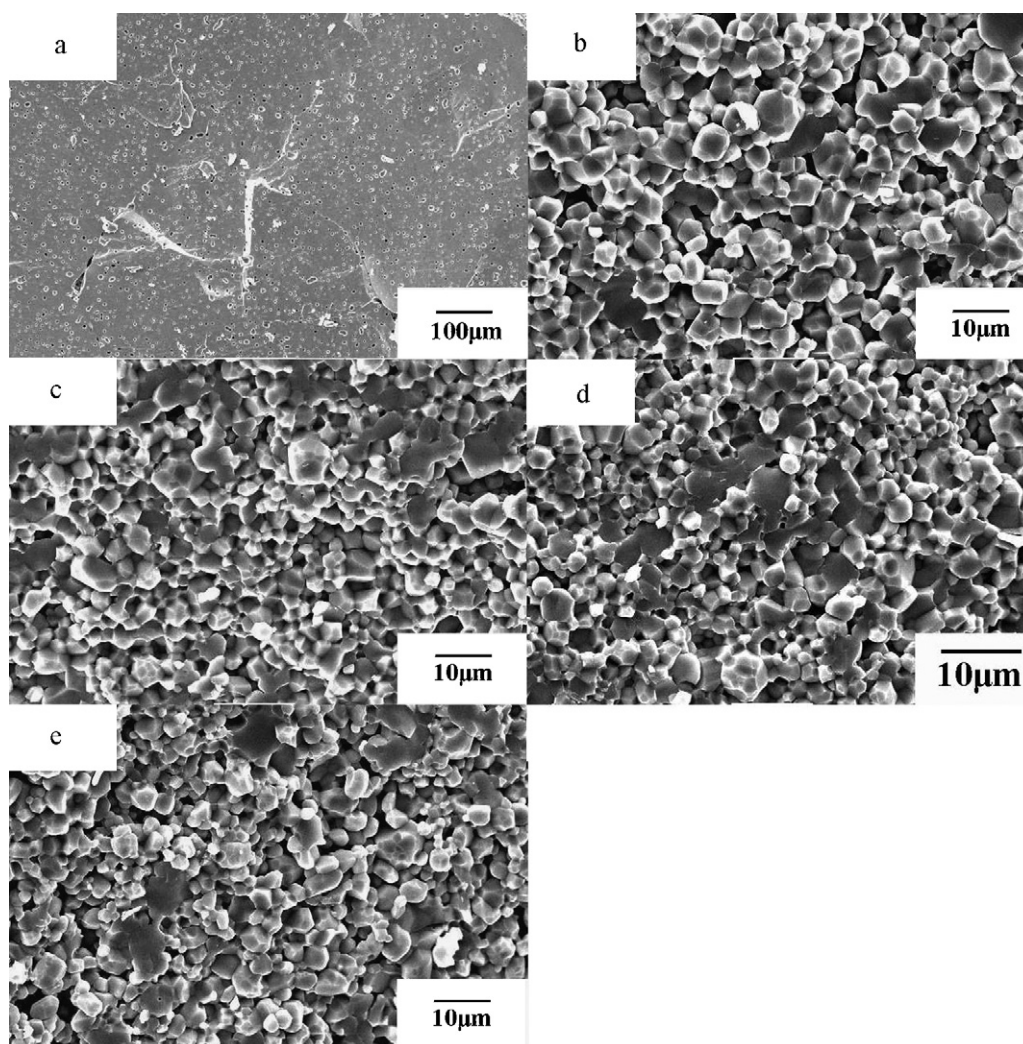


Fig. 2. SEM micrographs of (a) CCTO, (b) PCCTO-1, (c) PCCTO-2, (d) PCCTO-3 and (e) PCCTO-4.

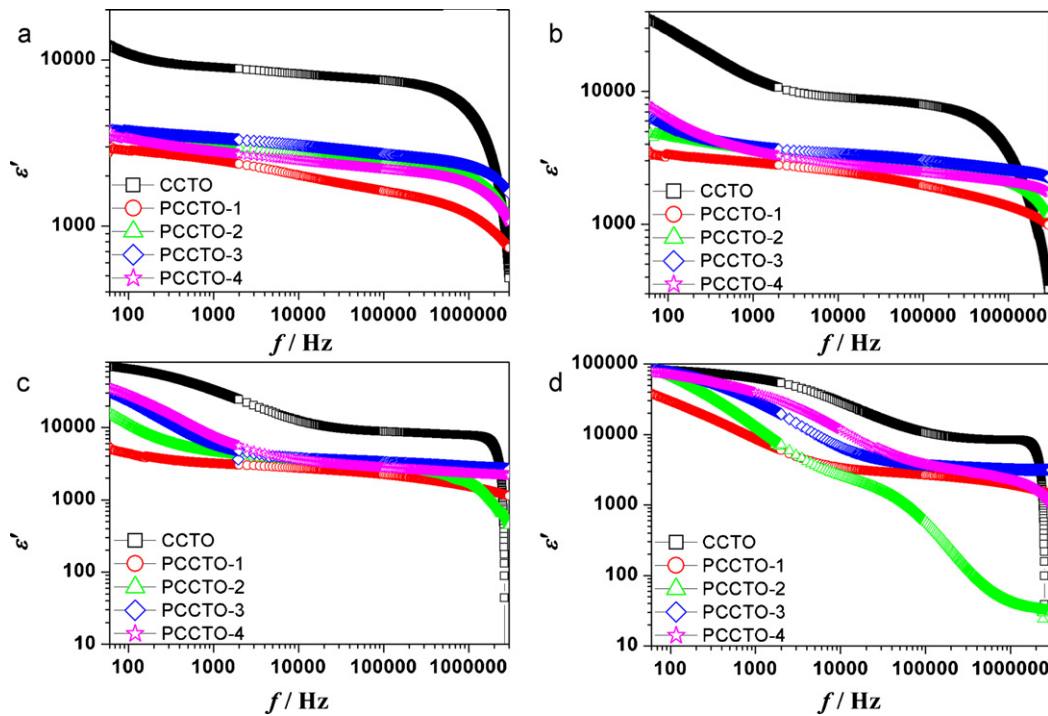


Fig. 3. Dielectric spectra of CCTO and PCCTOs ($x=0.05, 0.10, 0.15$ and 0.20) at selected temperature (a) 290 K, (b) 340 K, (c) 390 K and (d) 440 K.

(RT = 290 K) seen in Fig. 3(a), ϵ' are gradually larger with Pr doping amount increasing from 0.05 to 0.15, but this growth of dielectric constant would terminate at $x=0.15$. ϵ' values of all PCCTOs are almost an order of magnitude lower than that of pure CCTO ceramics. Here, mixing valence Pr-ion (Pr^{3+} and Pr^{4+}) would replace Ca^{2+} in CCTO grains as a donor dopant, which would make the grains n-type semiconductors: $\text{Pr}_6\text{O}_{11} \rightarrow 2\text{Pr}_{\text{Ca}}^{\bullet} + 4\text{Pr}_{\text{Ca}}^{\bullet\bullet} + 10\text{e}^- + 10\text{O}_x + 1/2\text{O}_2$. Afterwards, Ca^{2+} and oxygen atoms [5] would enter into the grain boundary as acceptors and make the grain boundaries p-type like features. Then double (back-to-back) Schottky potential barriers are created at the interfaces between n-type grains due to charge trapping at acceptor states, resulting in bending of the conduction band across the grain boundaries [16]. Pr_6O_{11} doping makes the acceptor concentration N_s at the grain boundaries increasing, in terms of the following Eq. (1). And then the Schottky potential Φ_b maybe enhanced which would result in a low dielectric constant by [5]:

$$\Phi_b = \frac{eN_s^2}{8\epsilon_0\epsilon_r N_d}, \quad (1)$$

where e is the electronic charge, N_s is the acceptor (surface charge) concentration, vacuum permittivity $\epsilon_0 = 8.854 \times 10^{-14}$ F/cm, ϵ_r is the relative permittivity of the material, and N_d is the charge carrier concentration in grains.

Besides, the dielectric spectra are flatter at frequencies of 10^2 – 10^6 Hz. For all doped and pure samples a sharp decreasing of ϵ' shows when the frequency gets higher than 10^6 Hz. The drastic decrease in ϵ' at frequencies higher than 10^6 Hz may indicate the presence of conductive grains [17]. Morrison et al. [18] had suggested an alternative mechanism, namely, oxygen-deficiency according to " $\text{O}^{2-} \rightarrow \text{V}_\text{O} + 1/2\text{O}_2 + 2\text{e}^-$ " was responsible for the conductivity. CCTO and all PCCTOs show an increase of ϵ' with increasing temperature, and the drop of the permittivity of PCCTOs has a large slope than pure CCTO. When the temperature is as higher as 440 K in Fig. 3(d), ϵ'_{max} are almost the same of 10^5 at 60 Hz for all doped and pure CCTO samples. The temperature dependent properties of the permittivity of CCTO could be related

to the excited deep trap states [19]. At low temperature the interface is static because of the large relaxation time τ . This relaxation time shrinks with increasing T and for $\omega\tau < 1$ the capacitance maybe enhanced by the dynamic interface.

Interestingly, the dependence of permittivity on frequency reveals the existence of two relaxation processes in high temperature range of 290–440 K. One is the low frequency relaxation, not completely visible in the frequency range of the available measurement at RT in Fig. 3(a), and the other is in the MHz region. The low frequency relaxation shows a step-like increasing of ϵ' with temperature rising, shifting to higher frequencies and behaving as the Debye-like relaxation. Due to the appearance of relaxation in low frequency range (below 10^4 Hz) at 390 K, it is presumed to be associated with surface layers interfacial polarization, and the similar results were reported by Prakash and Verma [20]. The low frequency relaxation is also observed in single-crystalline CCTO [21], which further suggests that the ϵ' plateau below 10^3 Hz which could be seen more clearly at 440 K should be related to surface layers in CCTO ceramics. And recently, Luo et al. [11] and Baerner et al. [12] et al. put forward that this low frequency relaxation is a trap state related relaxation, which could be changed by electric conditioning but recover after releasing electric field. Therefore, maybe the large permittivity in the low frequency range of CCTO could be attributed to the trap states which exist in the electrode surface. And because the time is long enough to let the traps response we could get a huge permittivity at low frequency. What is more, PCCTO-2 shows a middle frequency dielectric relaxation ($\sim 10^5$ Hz) at 440 K in Fig. 3(d), which may arise due to the hopping of trapped carriers at higher temperature. Higher temperature makes trapped charges in infirm interconnections of strongly distorted boundaries become carriers that redistribute at electrical heterogeneity regions [22], which results in a new dielectric relaxation with a very low dielectric constant.

Fig. 4 shows dielectric loss $\tan \delta$ of CCTO and PCCTOs dependent on frequencies in the temperature range of 290–440 K. Dielectric loss $\tan \delta$ are very small in the middle frequency range of 10^2 – 10^6 Hz and then sharply arise in the MHz region, which is

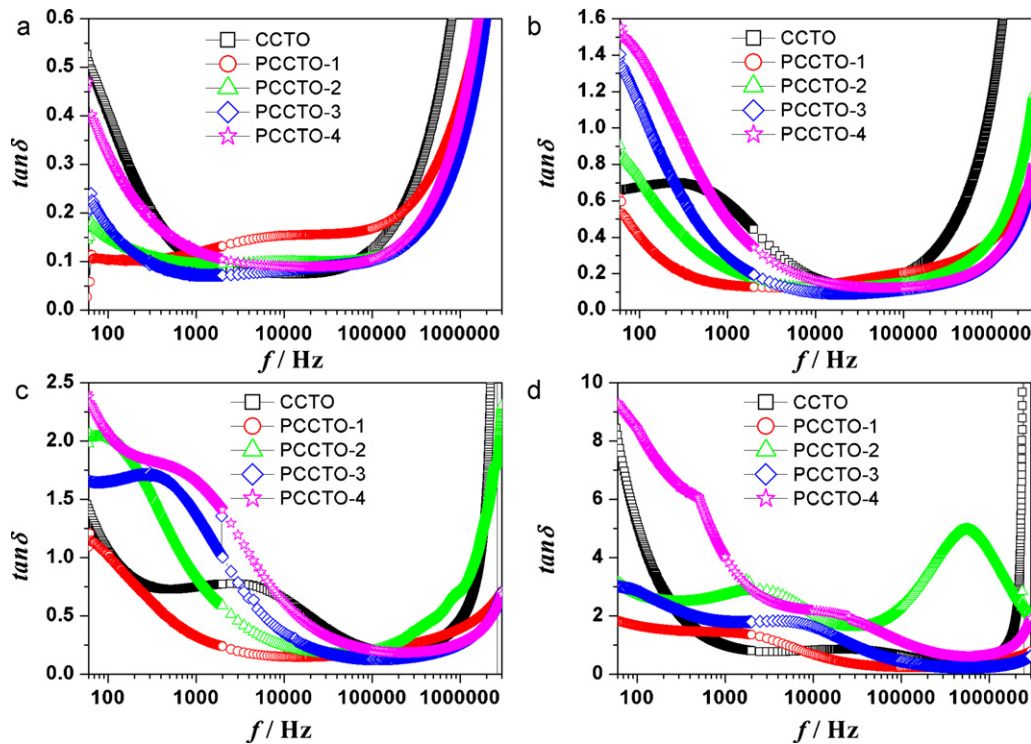


Fig. 4. Dielectric loss spectra of CCTO and PCCTOs ($x=0.05, 0.10, 0.15$ and 0.20) at selected temperature (a) 290 K, (b) 340 K, (c) 390 K and (d) 440 K.

caused by the n-type conductive grains as shown in the dielectric constant spectra in Fig. 3. A conspicuous increasing of $\tan \delta$ was found from RT to 440 K in all measured frequencies. With increasing x values from 0.05 to 0.20, the dielectric loss get bigger, but Pr doping can suppress the dielectric loss to some extent in the middle frequency range before 440 K. In the frequency range of 2×10^2 – 10^5 Hz, dielectric loss of PCCTOs are lower than 0.20 at RT. A low frequency (below 10^3 Hz) loss peak gradually comes up and moves to higher frequencies at the same time for each sample as temperature increasing, which could be caused by two relaxation segments competition of the electrode interfaces and grain boundaries at higher temperatures shown in Fig. 3. CCTO and all PCCTOs only show one peak in the measured temperature ranges except for PCCTO-2 ($x=0.10$), and the second peak at higher frequency (Fig. 4(d)) agrees well with its dielectric constant spectrum, which is caused by the high temperature relaxation of trapped carriers of the grain boundaries.

The complex impedance Z^* were modeled by an ideal equivalent circuit consisting of resistors R and capacitors C by ZView. Fig. 5

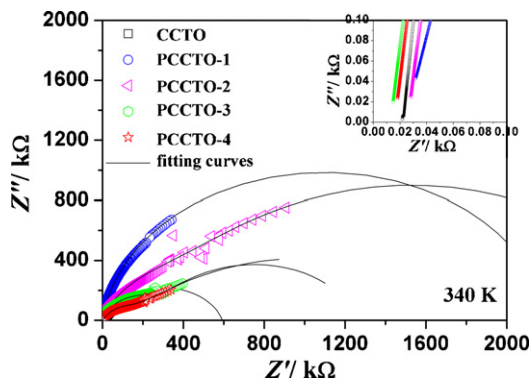


Fig. 5. Complex impedance Z^* spectra of CCTO and PCCTOs ($x=0.05, 0.10, 0.15$ and 0.20) at 340 K.

shows the typical measured and fitted complex impedance spectra of CCTO and all PCCTO samples at 340 K. Intercepts of Z' are not zero which corresponds well to the grain resistivity at high frequencies out of our measurements. And the other two semicircles imply a series array of two subcircuits, one representing grain boundary effects and the other representing electrode contact. Each subcircuit is composed of a resistor and a capacitor joined in parallel. By all fitted semicircles from 290 K to 490 K, the high temperature activation energies were calculated following the Arrhenius law and the expression can be described as [23]:

$$\tau = \tau_0 \exp\left(\frac{E_a}{k_B T}\right), \quad (2)$$

where τ_0 is the prefactor, E_a is the activation energy for the relaxation, k_B is Boltzmann constant, T is the absolute temperature, and the relaxation time $\tau = RC$. In Fig. 6 we plot $\ln \tau$ vs. $1000/T$, in which the solid lines are the fitted results using Eq. (2). From slopes of the fitted straight lines, the activation energies of two dielectric relaxations were calculated and shown in Table 1. As to pure CCTO

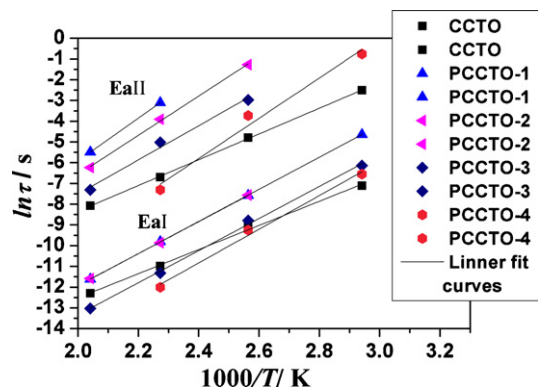


Fig. 6. Temperature dependence of relaxation time τ ($\ln \tau$ vs. $1000/T$) for dielectric relaxation I and II.

Table 1
Activation energies of CCTO and PCCTO ceramics.

Sample	CCTO	PCCTO-1	PCCTO-2	PCCTO-3	PCCTO-4
E_a I (eV)	0.5	0.67	0.66	0.67	0.7
E_a II (eV)	0.54	0.89	0.82	0.71	0.84

activation energies of E_a I (0.50 eV) and E_a II (0.54 eV) are in good agreement with the values of ~ 0.54 eV reported by Zhang of grain boundaries and electrodes, respectively [22]. From Table 1 we can see all doped CCTO samples have higher activation energies for the grain boundary and electrode contact than pure CCTO ceramics which is consistent with the higher Schottky potential Φ_b of PCCTOs as the former discussion in Fig. 3. Here more resistive grain boundary and electrode contact could be seen in Fig. 5, then causing a lower dielectric loss in low and middle frequency ranges at room temperature, respectively [24]. What is more, for PCCTOs, E_a II present a decreasing trend at first and increase in the end (for PCCTO-4), which corresponds well with the low frequency dielectric constant increasing firstly and decreasing as doping amount $x=0.20$ lastly. The above statements also assert that the low frequency platform (could be seen in Fig. 3(d)) were attributed to the electrode contact, especially the trap states in the deep energy level.

4. Conclusions

Pure and praseodymium doped CCTO samples were produced by conventional solid-state reaction method. From dielectric property measurements, XRD and SEM, we conclude that Pr doping can result in the grain size decreasing, which will lower the complex permittivity. From XRD, the third phase of Ca_2CuO_3 was observed with a higher concentration $x=0.20$. The Pr doping could make Ca^{2+} segregate to the grain boundary, which will promote resistivity, the grain boundary potential, and the significant changes of

activation energies of grain boundary and surface contact. Thereafter the dielectric constant and dielectric loss are decreased. From low to high frequency, three semicircles were observed corresponding to three different conducting regions: electrode interface, grain boundary and grain.

References

- [1] M.A. Subramanian, D. Li, N. Duan, B.A. Reisner, A.W. Sleight, J. Solid State Chem. 151 (2000) 323.
- [2] C.C. Homes, T. Vogt, S.M. Shapiro, S. Wakimoto, A.P. Ramirez, Science 293 (2001) 673.
- [3] L. Chen, C.L. Chen, Y. Lin, Y.B. Chen, X.H. Chen, R.P. Bontchev, C.Y. Park, A.J. Jacobson, Appl. Phys. Lett. 82 (2003) 2317.
- [4] S.M. Ke, H.T. Huang, H.Q. Fan, Appl. Phys. Lett. 89 (2006) 182904.
- [5] T.B. Adams, D.C. Sinclair, A.R. West, Phys. Rev. B 73 (2006) 094124.
- [6] D.C. Sinclair, T.B. Adams, F.D. Morrison, A.R. West, Appl. Phys. Lett. 80 (2002) 2153.
- [7] S.Y. Chung, I.D. Kim, S.J. Kang, Nat. Mater. 3 (2004) 774.
- [8] T.T. Fang, C.P. Liu, Chem. Mater. 17 (2005) 5167.
- [9] J.L. Zhang, P. Zheng, C.L. Wang, Appl. Phys. Lett. 87 (2005) 142901.
- [10] P. Lunkenheimer, R. Fichtl, S.G. Ebbinghaus, A. Loidl, Phys. Rev. B 70 (2004) 172102.
- [11] X.J. Luo, C.P. Yang, S.S. Chen, X.P. Song, H. Wang, K. Baerner, J. Appl. Phys. 108 (2010) 014107.
- [12] K. Baerner, X.J. Luo, X.P. Song, C. Hang, S.S. Chen, I.V. Medvedeva, C.P. Yang, J. Mater. Res. 26 (2011) 36.
- [13] P. Delugas, P. Alippi, V. Raineri, Mater. Sci. Eng. 8 (2010) 012015.
- [14] M.T. Buscaglia, M. Viviani, V. Buscaglia, C. Bottino, J. Am. Ceram. Soc. 85 (2002) 1569.
- [15] B.S. Prakash, K.B.R. Varma, J. Mater. Sci. 42 (2007) 7467.
- [16] J.J. Liu, C.G. Duan, W.N. Mei, R.W. Smith, J.R. Hardy, J. Appl. Phys. 98 (2005) 093703.
- [17] T.B. Adams, D.C. Sinclair, A.R. West, Adv. Mater. 14 (2002) 1321.
- [18] F.D. Morrison, D.C. Sinclair, A.R. West, Int. J. Inorg. Mater. 3 (2001) 1205.
- [19] G. Blatter, F. Greuter, Phys. Rev. B 33 (1986) 3952.
- [20] B.S. Prakash, K.B.R. Varma, J. Phys. Chem. Solids 68 (2007) 490.
- [21] S. Krohns, P. Lunkenheimer, S.G. Ebbinghaus, A. Loidl, J. Appl. Phys. 103 (2008) 084107.
- [22] L. Zhang, Appl. Phys. Lett. 87 (2005) 022907.
- [23] Y.H. Lin, J.N. Cai, M. Li, C.W. Nan, J.L. He, J. Appl. Phys. 103 (2008) 074111.
- [24] Y. Yan, L. Jin, L. Feng, G. Cao, Mater. Sci. Eng. B 130 (2006) 146.